The scaled boundary point interpolation method for seismic soil-tunnel interaction analysis

Mehran Hassanzadeh
Ph.D. Student, Department of Civil Engineering University of Tabriz, Iran
mehran.hassanzadeh@gmail.com

Hamid Reza Tohidvand
Research Assistant, Department of Civil Engineering University of Tabriz, Iran,
h.r.tohidvand@gmail.com

Masoud Hajialilue-Bonab
Corresponding author, Professor, Department of Civil Engineering, University of Tabriz, Tabriz, Iran Tel.: +98 41-33392551, hajialilue@tabrizu.ac.ir, mhbonab@gmail.com
Visiting Professor, Centre for Geotechnical Modeling, Department of Civil and Environmental Engineering, University of California at Davis, USA, Tel: +1-530-761-6210, mhbonab@ucdavis.edu

Akbar A. Javadi
Professor, Department of engineering, University of Exeter, Exeter EX4 4QF, Devon, UK.
a.a.javadi@ex.ac.uk

Abstract:

The scaled boundary method (SBM) is an effective numerical approach for analysing elastostatics of bounded and unbounded media. To enhance abilities of the scaled boundary approach, this method can be coupled with mesh free technology. In this paper a point interpolation based SBM is proposed to analyse seismic soil-tunnel interaction problem. In the proposed approach, boundary of domain is modelled with the scaled boundary point interpolation method while interior domain is modelled by the conventional finite element method (FEM). This is the first time that a mesh-free scaled boundary method is used to analyse seismic problems. The presented method has some advantages over previously presented mesh-free SBMs. In the scaled boundary point interpolation method, the shape functions have the Kronecker delta function property and do not require radial basis functions to discretize the boundary of 2D problems. A shaking table test is designed and used to verify the proposed method. It is shown that the proposed numerical approach leads to results that are in a good agreement with those of the designed shaking table tests.

Keywords: Scaled boundary method; Point interpolation; Mesh-free; Seismic analysis; Shaking table.

1. Introduction

Numerical analysis has been commonly used for solution of engineering problems in recent years. The conventional finite element method (FEM) is a powerful tool to investigate different problems. Another numerical approach that is used for analyzing engineering problems, is the finite difference method (FDM). For example, FDM can be applied to evaluate the critical factor of safety for underground rock caverns [2] or it can be used to analyze pillar stresses and interaction effects for twin rock caverns [3]. FEM and FDM are powerful tools for numerical investigations but they also have a number of limitations. These methods cannot be applied for analysis of unbounded media without extra assumptions. In addition, entire domain must be discretized in the FEM and FDM. Different numerical procedures can be found in the literature especially for solving tunnel engineering problems [4].

In recent years, the conventional boundary element method (BEM) has been applied to analyze different engineering problems. Seepage, [5, 6] static [7, 8] and dynamic problems [9, 10] were analyzed by the BEM successfully. The boundary element method requires a fundamental solution which must satisfy the governing equations in the domain of the problem exactly [11]. Calculating the fundamental solution for different problems can be a very time consuming procedure. In the past two decades, Wolf and Song [12] developed a boundary element approach that does not require a fundamental solution. This method, which is named scaled boundary method, is a semi analytical method and couples the advantages of the two mostly used finite element (FE) and boundary element methods [13]. In the scaled boundary method (SBM), by using a scale center (SC) and two dimensionless local coordinates (η, ξ) (for two-dimensional (2D) problems) the governing equations can be transformed to a new coordinate system. The scheme for domain discretization of the scaled boundary method is

shown in Fig. 1.

Like the boundary element method, the scaled boundary method has been applied to solve different problems. For example, this method has been used to analyze seepage [14, 15], static [16, 17] and dynamic problems [18, 19].

For seismic analysis, Junyi and his coworkers [20] proposed a free field input model based on the coupled scaled boundary finite element-finite element (SBFE-FE) method in time domain. Genes and Kocak [21] used the SBFE-FE method to analyze seismic soil structure interaction problems. Nonlinear seismic investigation was carried out in [22] to predict building responses to earthquake loading. Seiphoori et al. [23] used the SBFE-FE method for three-dimensional analysis of concrete rock fill dams. Bazyar and Basirat [24] detailed the formulation of the SBFEM to investigate seismic problems. Tohidvand and Hajialilue-bonab [25] carried out a seismic soil-structure interaction analysis using the coupled scaled boundary spectral element-spectral element method. They used an adaptive method to calculate acceleration unit impulse matrix in seismic loading condition. All of the above mentioned seismic analyses were evaluated by mesh-based scaled boundary approaches.

To enhance the capabilities of the scaled boundary approach, researchers have applied a number of different modifications. An improvement can be applied by combining virtues of the mesh-free technology and the scaled boundary approach. In the boundary type mesh-free methods, discretization is only required in the boundary of the problem, so the number of degrees of freedoms (DOFs) required to solve problems can be decreased significantly. One of the first boundary type mesh-free methods proposed in the literature is the boundary node method (BNM) that was presented by Mukherjee and Mukherjee in 1997 [26]. Zhu and Atluri [27] presented the local boundary integral equation (LBIE) method. Both of the BNM and LBIE

utilize the moving least squares (MLS) approximation to construct shape functions and their derivatives. Therefore, these methods cannot satisfy the Kronecker delta function property. The boundary point interpolation method (BPIM) was proposed by Liu and Gu [28] to analyze engineering problems. The boundary point interpolation method uses the point interpolation technique to construct shape functions, so shape functions have the Kronecker delta function property.

Two mesh-free versions of the scaled boundary method, based on the mesh-free Local Petrov–Galerkin approach and element-free Galerkin approach, were presented by Deeks and Augarde [29] and He et al. [30]. These methods use MLS approximation in their formulations. The radial point interpolation based scaled boundary method (RPISBM) was recently used by different researchers to solve engineering problems. Fracture analysis of piezoelectric material [31], crack problem [32] and two dimensional elasto-static problems [33] were investigated by RPISBM. For two-dimensional problems, as the boundary acts like a continuous line in the mapped form, there is no need to use radial functions in constructing of shape functions. In other words, singularity cannot occur in point interpolation based boundary shape functions. In this paper an efficient scaled boundary method is presented by using the point interpolation technique. The advantages of the proposed method in comparison with previously presented methods are:

(1) Scaled boundary point interpolation method (SBPIM) discretizes only the boundary of the problem, so the dimension of the problem can be reduced by one.

(2) Scaled boundary point interpolation method uses polynomial basis to determine shape functions and these shape functions have Kronecker delta function property. This feature makes the SBPIM more efficient than the element-free Galerkin or the local Petrov Galerkin based

boundary methods.

(3) SBPIM uses only the polynomial basis in shape functions, so computational efforts for calculating radial basis are removed.

As mentioned above, the scaled boundary point interpolation method has some benefits that make this method more efficient than previously presented scaled boundary approaches. SBPIM does not use bell shape weight functions, therefore this method cannot ensure the compatibility feature for nodes in the global domain when a local support domain is used. To model bounded media, a radial basis point interpolation method is used in this paper. In this research, the coupled SBPIM-FEM is used to analyze seismic soil tunnel interaction problems.

The paper is organized as follows: The basic equations of the scaled boundary point interpolation method are detailed in the next section. A number of example problems are solved in Section 3 to verify the methodology and to show the efficiency of the proposed approach. A shaking table test is designed and used to analyze wave propagation problems and the results of the coupled SBPIM-FEM are verified against the experimental data.

2. Scaled boundary point interpolation method

The fundamental solution-less scaled boundary method is a semi-analytical method which solves boundary value problems numerically in circumferential direction and analytically in radial direction [12]. This method transforms the governing partial differential equation to a set of ordinary differential equations (Cauchy–Euler differential equations in static problems). In the SBM boundary of the domain is discretized with respect to a scale center. This scale center with coordinates (x_0, y_0) must be selected in such manner that all of the boundary can be seen from it (Fig. 1). The essence of the scaled boundary method is mapping of Cartesian coordinate system to the scaled boundary coordinate system. For each point in the boundary of the domain it can be

stated that

$$x(\xi) = x_0 + \xi\, x(\eta) \tag{1}$$

$$y(\xi) = y_0 + \xi\, y(\eta) \tag{2}$$

where ξ is the radial coordinate and η is the circumferential coordinate. An approximation of field variable can be defined using Eq. (3).

$$\{u_h(\xi,\eta)\} = [N_h(\eta)]\{u_h(\xi)\} \tag{3}$$

In Eq. (3) $N_h(\eta)$ is matrix of shape functions. $u_h(\xi)$ is a set of n functions of ξ [30]. Strains in Cartesian coordinate system can be calculated using Eq. (4).

$$\{\varepsilon_h(\xi,\eta)\} = [L].\{u_h(\xi,\eta)\} \tag{4}$$

As the boundary of the domain is mapped to the scaled boundary coordinate system, to calculate stains in the new system, a new operator (L^*) instead of the conventional differential operator L must be used. This new operator is defined in the form:

$$[L^*] = [b^1(\eta)]\frac{\partial}{\partial\xi} + \frac{1}{\xi}[b^2(\eta)]\frac{\partial}{\partial\eta} \tag{5}$$

where $[b^1(\eta)]$ and $[b^2(\eta)]$ are functions of coordinates and shape functions. These matrices can be calculated using Eq. (6) and Eq. (7).

$$[b^1] = \frac{1}{|\,jac\,|}\begin{bmatrix} y(\eta),\eta & 0 \\ 0 & -x(\eta),\eta \\ -x(\eta),\eta & y(\eta),\eta \end{bmatrix} \tag{6}$$

$$[b^2] = \frac{1}{|\,jac\,|}\begin{bmatrix} -y(\eta) & 0 \\ 0 & x(\eta) \\ x(\eta) & -y(\eta) \end{bmatrix} \tag{7}$$

In these equations, $|jac|$ is the Jacobian of the support domain and can be determined as:

$$| jac | = x(\eta) y(\eta),_{\eta} - y(\eta) x(\eta),_{\eta} \tag{8}$$

In Eq. (8), x, y, and their derivatives can be determined as follows:

$$x(\eta) = [N_1(\eta) \quad N_2(\eta) \quad N_3(\eta).....N_N(\eta)] \begin{Bmatrix} x_1 \\ x_2 \\ \text{M} \\ x_n \end{Bmatrix} \tag{9}$$

$$y(\eta) = [N_1(\eta) \quad N_2(\eta) \quad N_3(\eta).....N_N(\eta)] \begin{Bmatrix} y_1 \\ y_2 \\ \text{M} \\ y_n \end{Bmatrix} \tag{10}$$

$$x(\eta),\eta = [N_1(\eta) \quad N_2(\eta) \quad N_3(\eta).....N_N(\eta)],\eta \begin{Bmatrix} x_1 \\ x_2 \\ \text{M} \\ x_n \end{Bmatrix} \tag{11}$$

$$y(\eta),\eta = [N_1(\eta) \quad N_2(\eta) \quad N_3(\eta).....N_N(\eta)],\eta \begin{Bmatrix} y_1 \\ y_2 \\ \text{M} \\ y_n \end{Bmatrix} \tag{12}$$

In this paper, the point interpolation method (PIM) is used to create shape functions and their derivatives. The point interpolation method uses polynomial basis in the interpolation functions. By considering a support domain with n nodes (for example 6 nodes in Fig. 2) to interpolate field variable ($u(\eta)$), Eq. 13 can be considered as the starting point of the PIM formulation.

$$u(\eta) = [p_1(\eta) \quad p_2(\eta) \quad p_3(\eta).....p_n(\eta)] \begin{Bmatrix} a_1 \\ a_2 \\ \text{M} \\ a_n \end{Bmatrix} = P^T a \tag{13}$$

Where the coefficient a_i is the *ith* unknown coefficient and p_j is the *jth* monomial. As the scaled boundary method only models the boundary of domain, the dimension of the problem is reduced

by one. Therefore, one dimensional monomials are sufficient in this study. The number of monomials should be equal to the number of nodes in the PIM. Eq. (14) shows the vector of monomials for a 1D boundary:

$$p^T(\eta) = [1 \;\; \eta^1 \;\; \eta^2 \;\; ..... \;\; \eta^{n-1}] \tag{14}$$

In order to calculate the unknown coefficients a_i in Eq. (13), field variable $u(\eta)$ can be enforced in Eq. (13) to pass nodal values [34]. So, n equations for each node can be constructed. The resulted system of equations can be written in a matrix form as:

$$U_s = P_m a \tag{15}$$

where P_m is the moment matrix and can be defined as

$$p_m = \begin{bmatrix} 1 & \eta_1 & \eta_1^2 & \text{K} & \eta_1^{n-1} \\ 1 & \eta_2 & \eta_2^2 & \text{K} & \eta_2^{n-1} \\ 1 & \eta_3 & \eta_3^2 & \text{K} & \eta_3^{n-1} \\ \text{M} & \text{M} & \text{M} & \text{O} & \text{M} \\ 1 & \eta_n & \eta_n^2 & \Lambda & \eta_n^{n-1} \end{bmatrix} \tag{16}$$

Solving Eq. (15) for the unknown vector a leads to

$$a = P_m^{-1} U_s \tag{17}$$

For one dimensional problems, p_m^{-1} always exists. However, for 2D problems, singularity can occur.

Substituting Eq. (17) back into Eq. (13) yields:

$$u(\eta) = p^T(\eta) P_m^{-1} U_s = \{N\} U_s \tag{18}$$

where N is a vector of shape functions and can be defiend as

$$N = p^T(\eta) P_m^{-1} = \{N_1 \;\; N_2 \;\; .....N_n\} \tag{19}$$

The derivatives of the PIM shape functions can be easily obtained by using Eq. (20).

$$\frac{dN(\eta)}{d\eta} = \frac{dp^T(\eta)}{d\eta} P_m^{-1} \tag{20}$$

By substituting Eq. (3) and (5) in Eq. (4) it can be found that

$$\begin{aligned}\{\varepsilon_h(\xi,\eta)\} = [L^*]\{u_h(\xi,\eta)\} = [L^*][N_h(\eta)]\{u_h(\xi)\} = \\ [B^1(\eta)]\{u_h(\xi)\}_{,\xi} + \frac{1}{\xi}[B^2(\eta)]\{u_h(\xi)\}\end{aligned} \tag{21}$$

B^1 and B^2 can be obtained using equations (22) and (23).

$$[B^1(\eta)] = [b^1(\eta)][N(\eta)] \tag{22}$$

$$[B^2(\eta)] = [b^2(\eta)][N(\eta)]_{,\eta} \tag{23}$$

By multiplying equation (21) in elasticity matrix (D), stresses can be found.

$$\begin{aligned}\{\sigma_h(\xi,\eta)\} = [D]\,[B^1(\eta)]\{u_h(\xi)\}_{,\xi} \\ + \frac{1}{\xi}[D][B^2(\eta)]\{u_h(\xi)\}\end{aligned} \tag{24}$$

The principle of virtual work (by ignoring the effect of body force) can be written as:

$$\int_v \{\delta\varepsilon(\xi,\eta)\}^T \{\sigma_h(\xi,\eta)\} dV - \int_s \{\delta u(\eta)\}^T \{t(\eta)\} dS = 0 \tag{25}$$

In Eq. (25), $\{\delta u(\eta)\}$ is the virtual displacement field and $\{\delta \varepsilon (\xi, \eta)\}$ is the virtual strain field. The first term is the internal work and the second term is the external work. By substituting Eq. (21) in the first term of Eq. (25) and using some mathematical manipulation, the expression for internal work can be written as:

$$\{\delta \mathrm{u}\}^{\mathrm{T}}\left([\mathrm{E}^{0}]\{\mathrm{u}_{\mathrm{h}}\}_{,\xi}+[\mathrm{E}^{1}]^{\mathrm{T}}\{\mathrm{u}_{\mathrm{h}}\}\right)-\int_{0}^{1}\{\delta \mathrm{u}(\xi)\}^{\mathrm{T}}\begin{pmatrix}[\mathrm{E}^{0}]\xi\{u_h(\xi)\}_{,\xi\xi}+\\ \left[[\mathrm{E}^{0}]+[\mathrm{E}^{1}]^{\mathrm{T}}-[\mathrm{E}^{1}]\right]\{u_h(\xi)\}_{,\xi}\\ -[E^{2}]\frac{1}{\xi}\{u_h(\xi)\}\end{pmatrix}d\xi \quad (26)$$

In the above equation, E^0, E^1 and E^2 are coefficient matrices of the scaled boundary method and have the form

$$[E^{0}]=\int_{-1}^{+1}[B^{1}]^{T}[D][B^{1}]\,|\,J\,|\,d\eta \quad (27)$$

$$[E^{1}]=\int_{-1}^{+1}[B^{2}]^{T}[D][B^{1}]\,|\,J\,|\,d\eta \quad (28)$$

$$[E^{2}]=\int_{-1}^{+1}[B^{2}]^{T}[D][B^{2}]\,|\,J\,|\,d\eta \quad (29)$$

In the above equations [D] and [ρ] are elasticity and density matrices respectively. It should be noted that |J| in Eqs. (27-29) is not the same as |jac| in Eq. (6-7). |jac| is the Jacobian of support domain while |J| is Jacobian of integration cell.

The second term of the principle of virtual work can be obtained as:

$$\int_{S}\{\delta u(\eta)\}^{T}\{t(\eta)\}ds=\{\partial u\}^{T}\int_{s}[N(\eta)]\{t(\eta)\}ds=\{\partial u\}^{T}\{p\} \quad (30)$$

Therefore, the full expression of the principle of virtual work can be written as:

$$\begin{aligned}&\{\delta u\}^{T}\left([E^{0}]\{u_h\}_{,\xi}+[E^{1}]^{T}\{u_h\}\right)-\{\delta u\}^{T}\{p\}-\\&\int_{0}^{1}\{\delta u(\xi)\}^{T}\left([E^{0}]\xi\{u_h(\xi)\}_{,\xi\xi}+\left[[E^{0}]+[E^{1}]^{T}-[E^{1}]\right]\{u_h(\xi)\}_{,\xi}-[E^{2}]\frac{1}{\xi}\{u_h(\xi)\}\right)d\xi=0\end{aligned} \quad (31)$$

By setting virtual displacement equal to zero, two equations can be obtained; one of them is a second order differential equation (Eq. (32)) that is called the scaled boundary equation in displacements.

$$[\mathrm{E}^0]\xi^2\{u_h(\xi)\}_{,\xi\xi}+\left[[\mathrm{E}^0]+[\mathrm{E}^1]^{\mathrm{T}}-[\mathrm{E}^1]\right]\{u_h(\xi)\}_{,\xi}-[E^2]\{u_h(\xi)\}=0 \tag{32}$$

For dynamic or seismic loading cases, the equation of motion can be written as:

$$\begin{bmatrix} k_{ii} & k_{i\Gamma} \\ k_{\Gamma i} & k_{\Gamma\Gamma} \end{bmatrix}\begin{bmatrix} u_i(t) \\ u_\Gamma(t) \end{bmatrix}+\begin{bmatrix} C_{ii} & C_{i\Gamma} \\ C_{\Gamma i} & C_{\Gamma\Gamma} \end{bmatrix}\begin{bmatrix} v_i(t) \\ v_\Gamma(t) \end{bmatrix}+\begin{bmatrix} M_{ii} & M_{i\Gamma} \\ M_{\Gamma i} & M_{\Gamma\Gamma}+\gamma\Delta t M_0^{\infty} \end{bmatrix}\begin{bmatrix} a_i(t) \\ a_\Gamma(t) \end{bmatrix}=\begin{bmatrix} p_i(t) \\ p_\Gamma(t)-r_\Gamma(t) \end{bmatrix} \tag{33}$$

where [*M*], [*C*] and [*K*] are mass, damping and stiffness matrices respectively and {*a*}, {*v*} and {*u*} are acceleration, velocity and displacement vectors. The subscript *Γ* indicates degrees of freedom of the nodes on the near and far field interface. The subscript (*i*) denotes degrees of freedom on the remaining nodes of the structure. In this equation, {*r*Γ} is the interaction force vector and for seismic loading case can be calculated as:

$$r(t)=\int_0^t M^{\infty}(t-\tau)\{a(\tau)-a_g(\tau)\}d\tau \tag{34}$$

where $M^{\infty}(t)$ is the acceleration unit impulse response matrix and a_g is the seismic acceleration.

3. Numerical verifications

In this section, two numerical examples are presented to show the accuracy and efficiency of the proposed scaled boundary point interpolation method to analyze soil structure interaction problems. The accuracy of the method is investigated by solving two wave propagation problem.

3.1- An elastic half space subjected to Ricker wavelet type dynamic load

In this example, to analyze wave propagation in unbounded soil media, an elastic half space is considered. The elastic half space on Cartesian coordinate system is shown in Fig. 3a. This half space has a Young's modulus E=2.66×10^5 kN/m^2, Poisson's ratio v=0.33 and a mass density ρ=2×10^3 kg/m^3. Fig. 3a also shows the details of loading and observation points. Fig. 3b shows the distribution of nodes in the considered domain and Fig. 3c shows a Ricker wavelet type dynamic load which is applied to the domain, horizontally.

In order to model the bounded medium, the conventional finite element method is used. A coupled SBPIM-FEM is used to evaluate the problem. The result of a coupled boundary element-finite element (BE-FE) method extracted from [35] are used to verify the obtained results. The results of the calculated horizontal displacement of point A are shown for both of the above mentioned approaches in Fig.4. It is shown that an excellent agreement has been achieved between the coupled SBPIM-FEM and BE-FE approaches.

3.2- An elastic half space subjected to a vertical dynamic load

A rectangular soil medium subjected to a vertical dynamic load is considered in this example. Fig. 5a shows the considered medium and the applied dynamic load. The finite element mesh used is shown in Fig. 5b. The considered half space has elastic modulus E=1.77 ×10^7 kN/m^2 and shear wave velocity equal to 4.74×10^2 m/s. The load intensity is equal to 68980 kN/m. The results of the proposed SBPIM-FEM are compared with the results of the boundary element method extracted from the literature [36]. The comparison of the results is shown in Fig. 5c. It is shown that an excellent agreement is obtained between the two methods. To ensure the accuracy of the proposed SBPIM-FEM in other parameters, acceleration time history of points B and C are calculated by the scaled boundary finite element- finite element method. Then the results are

compared with the SBPIM-FEM in Fig. 6a and Fig. 6b. It is shown that the two mentioned methods have excellent agreements with each other.

4. Numerical and experimental study

Fast population growth in large cities, as a global phenomenon, has led to a serious shortage of above ground space, and has therefore led to the development of underground structures such as metro transportation lines. Construction and development of underground transportation lines like metro tunnels in urban areas is a suitable choice to reduce volume of traffic especially in large cities. Seismic response analysis of these tunnels has attracted increasing attentions in recent years.

For this section, a shaking table test was designed to verify the proposed scaled boundary point interpolation method. A rectangular tunnel with rigid lining is considered. Fig. 7 shows the shaking table apparatus and the shear box used for this test.

The soil container used in the study is a laminar shear box with overall dimensions of 1.32 m length (x), 0.86 m width (y) and 0.82 m height (z). The soil container was constructed by 21 steel frames stacked on each other. To model rigid lining, an aluminum box with a high elastic modulus is used (Fig. 8).

Shear wave velocity of the soil in the used model is evaluated by a hammer test and mass density of the soil is determined directly from the constructed model. The material properties of the surrounding soil in the model are defined by the shear wave velocity vs=50 m/s, Poisson's ratio v=0.3 and mass density ρ=1.55 ton/m3. Table 1 shows values of material properties for the considered model.

Table. 1. Material properties for the considered model

Material property	-
Mass density (ton/m3)	1.55
Shear wave velocity (m/s)	50

As the scaled boundary method is able to evaluate wave propagation problems, only a small part of the soil medium is modeled. In addition, because of the symmetry, only half of the system is modelled. Fig. 9 shows the geometry of the system which is used in the investigation.

The model is subjected to a periodic base shaking. The acceleration time history of the applied vibration is shown in Fig. 10a.

The resulted horizontal displacement of point A is shown in Fig. 10b and the horizontal acceleration of this point is shown in Fig. 10c. A good agreement is observed between the results of the experimental tests and the SBPIM-FEM method. Fourier amplitudes of displacements for both the numerical and experimental models are shown in Fig. 11. The figure shows a good agreement between the results.

For another verification, a different acceleration time history is applied to the apparatus. The time history of the selected acceleration is shown in Fig. 12a. The resulted displacement and acceleration time histories are shown in Figs. 12b and 12c, respectively. As the figures indicate, a good agreement is observed between the experimental and the SBPIM-FEM results.

As a further verification using the shaking table test, another acceleration time history is used. Fig 13a shows the selected time history of acceleration. The resulted acceleration and displacement time histories of point A are shown in Figs. 13b and 13c respectively. Again an excellent agreement is observed between the experimental and numerical results.

5. Discussion and conclusion

In this paper, a mesh-free scaled boundary point interpolation method was presented to analyze seismic soil structure interaction problems. Like other scaled boundary approaches, no fundamental solution is needed in SBPIM. The point interpolation method uses only polynomial basis in its formulation. There is no need to add radial basis in the 2D scaled boundary method. To model bounded media, the conventional finite element method is employed. The application of the proposed mesh-free scaled boundary approach was illustrated using two numerical examples. An excellent agreement was achieved between the results of the proposed model and the other numerical approaches. A final verification was presented by using an experimental study. The results of the coupled SBPIM-FEM were compared with those of a shaking table test and a good agreement was obtained between them. It can be concluded that the proposed method can model seismic soil tunnel interaction problems with a very high accuracy.

References

1- Chhenga Ch. and Likitlersuangb S. Underground excavation behaviour in Bangkok using three-dimensional finite element method, Computers and Geotechnics, 2018; 95: 68-81.

2- Zhang W and Goh A. Reliability assessment on ultimate and serviceability limit states and determination of critical factor of safety for underground rock caverns, Tunnelling and Underground Space Technology, 2012; 32: 221-230.

3- Zhang W and Goh A. Numerical study of pillar stresses and interaction effects for twin rock caverns, International Journal for Numerical and Analytical Methods in Geomechanics, 2015; 39:193–206.

4- Lu Q, Sun HY and Low BK. Reliability analysis of ground support interaction in circular tunnels using the response surface method, International Journal of Rock Mechanics & Mining Sciences 2011; 48: 1329–1343.

5. Rafiezadeh K and Ataie-Ashtiani B. Transient free-surface seepage in three-dimensional general anisotropic media by BEM, Engineering Analysis with Boundary Elements, 2014; 46: 51-66.

6. Rafiezadeh K and Ataie-Ashtiani B. Three dimensional flow in anisotropic zoned porous media using boundary element method, Engineering Analysis with Boundary Elements, 2016; 36: 812–824.

7. Ribeiro DB and Paiva JB. A new BE formulation coupled to the FEM for simulating vertical pile groups, Engineering Analysis with Boundary Elements, 2014;41: 1–9.

8. Gaspari D and Aristodemo M. Torsion and flexure analysis of orthotropic beams by a boundary element model, Engineering Analysis with Boundary Elements, 2005; 29: 850-858.

9. Pak RYS and Guzina BB. Seismic soil-structure interaction analysis by direct boundary element methods, International Journal of Solids and Structures, 1999;36: 4743-4766.

10. Hamzehei-Javaran S and Khaji N. Dynamic analysis of plane elasticity with new complex Fourier radial basis functions in the dual reciprocity boundary element method, Applied Mathematical Modelling, 2014; 38: 3641-3651.

11. Wolf JP. The scaled boundary finite element method, John Wiley & Sons, UK. 2003.

12. Wolf JP and Song Ch. Finite-element modeling of unbounded media. John Wiley & Sons, Chichester. 1996.

13. Deeks AJ and Wolf JP. A virtual work derivation of the scaled boundary finite-element method for elastostatics, Computational Mechanics, 2002; 28: 489-504.

14. Bazyar MH, and Talebi A. Transient seepage analysis in zoned anisotropic soils based on the scaled boundary finite-element method, International Journal for Numerical and Analytical Methods in Geomechanics, 2014; 39 (1); 1-12.

15. Bazyar MH, and Graili A. Scaled boundary finite element solution to confined seepage problems. Journal of computational methods in engineering (Esteghlal), 2011; 30 (1): 61-78.

16. Lin G, Zhang Y, Hu ZQ, Zhong H. Scaled boundary isogeometric analysis for 2D elastostatics, Science China Physics. Mechanics and Astronronomy, 2014**;** 57: 286-300.

17. Long XY, Jiang C, Han X, Gao W, Bi RG. Sensitivity analysis of the scaled boundary finite element method for elastostatics, Computational Methods in Applied Mechanics and Engineering, 2014; 276: 212-232.

18. Song Ch, Wolf JP. The scaled boundary finite element method-alias consistent infinitesimal finite element cell method for elastodynamics. Computational Methods in Applied Mechanics and Engineering, 1997; 147: 329-355.

19. Hajialilue-Bonab M, and Tohidvand HR. A modified scaled boundary approach in frequency domain with diagonal coefficient matrices. Engineering Analysis with Boundary Elements, 2015**;** 50: 8-18.

20. Junyi Y, Feng J, Yanjie X. A seismic free field input model for FE-SBFE coupling in time domain, Earthquake Engineering and Engineering Vibration, 2003; 2(1): 51-58.

21. Genes MC, Kocak S. Seismic analyses of soil structure interaction system by coupling the finite element and the scaled boundary finite element methods, International symposium on structural and earthquake engineering. Middle East technical university. 2002.

22. Celebi E, Goktepe F, Karahan N. Non-linear finite element analysis for prediction of seismic response of buildings considering soil-structure interaction, Natural Hazards and Earth System Sciences, 2012**;** 12: 3495-3505.

23. Seiphoori A, Haeri M, Karimi M. Three dimensional nonlinear seismica nalysis of concrete faced rock fill dams subjected to scattered P, SV, and SH waves considering the dam–foundation interaction effects, Soil Dynamics and Earthquake Engineering, 2011**;** 31: 792-804.

24. Bazyar MH, Basirat B. Dynamic Soil-Structure Interaction Analysis under Seismic Loads Using the Scaled Boundary Finite-Element Method, Journal of Seismology and Earthquake Engineering 2012; 14 (1): 57-68.

25. Tohidvand HR, Hajialilue-Bonab M. Seismic soil structure interaction analysis using an effective scaled boundary spectral element approach, Asian Journal of Civil Engineering, 2014**;** 15: 501-516.

26. Mukherjee YX, Mukherjee S. Boundary node method for potential problems, International Journal for Numerical Methods in Engineering, 1997; 40: 797-815.

27. Zhu T, Atluri SN. A modified collocation and a penalty formulation for enforcing the essential boundary conditions in the element free Galerkin method, Computational Mechanics, 1998; 21: 211-222.

28. Liu GR, Gu YT. Coupling of element free Galerkin and hybrid boundary element methods using modified variational formulation, Computational Mechanics, 2000; 26(2): 166-173.

29. Deeks AJ, Augarde CE. A mesh less local Petrov–Galerkin scaled boundary method, Computational Mechanics. 2005; 36: 159–170.

30. He Y, Yang H, Deeks AJ. An Element free Galerkin (EFG) scaled boundary method, Finite Elements in Analysis and Design, 2012; 62: 28-35.

31. Chen SS, Wang J, Li QH. Two-dimensional fracture analysis of piezoelectric material based on the scaled boundary node method, Chinese Physics, 2016; 25(4): 1-8.

32. Chen SS, Li QH, Liu YH. Scaled boundary node method applied to two-dimensional crack problems, Chinese Physics, 2012; 21(11): 1-9.

33. Hajiazizi M, Graili A. A scaled boundary radial point interpolation method for 2-D elasticity problems, doi: 10.1002/nme.5534. 2017.

34. Liu GR. and Gu YT. An introduction to mesh-free methods and their programming, Springer. 2005.

35. Lehmann L. An effective finite element approach for soil-structure analysis in the time-domain Structural Engineering and Mechanics, Structural Engineering and Mechanics, 2005**;** 21(4): 1-14.

36. Estorff O, Firuzian M. Coupled BEM/FEM approach for nonlinear soil/structure interaction. Engineering analysis with boundary elements, 2000; 24: 715-725.

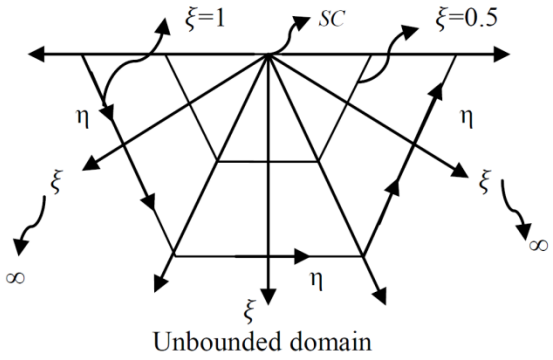

Fig.1. Domain discretization scheme of the scaled boundary method.

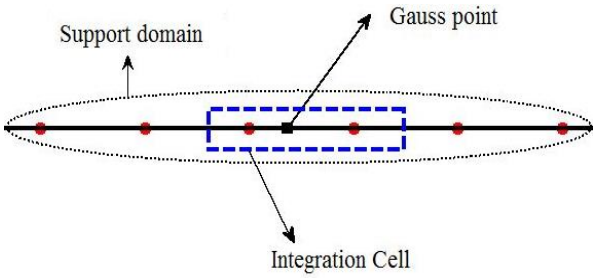

Fig.2. Support domain of a Gauss point in scaled boundary point interpolation method.

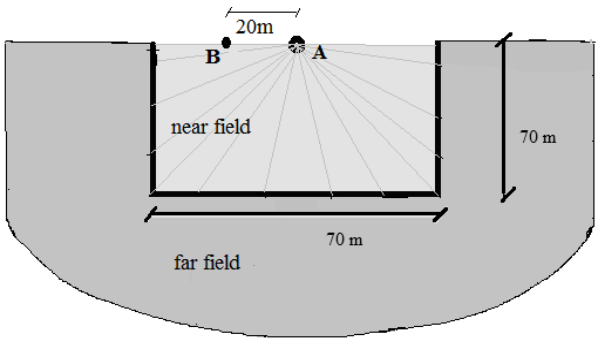
20m
B
A
near field
70 m
70 m
far field

(a)

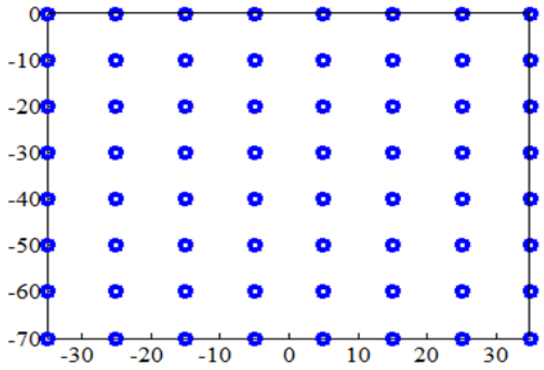
0
-10
-20
-30
-40
-50
-60
-70
-30
-20
-10
0
10
20
30

(b)

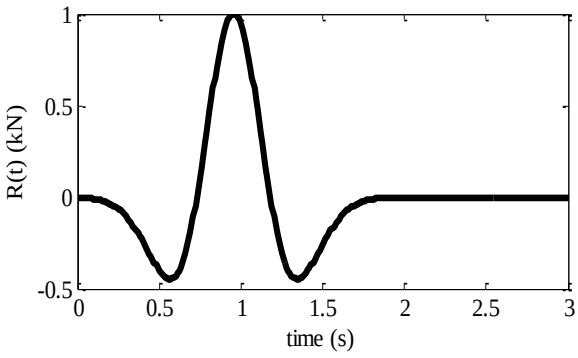
1
0.5
0
-0.5
R(t) (kN)
0
0.5
1
1.5
2
2.5
3
time (s)

(c)

Fig. 3 (a) Considered elastic half space (b) Distribution of nodes in the domain (c) Time history of the load function.

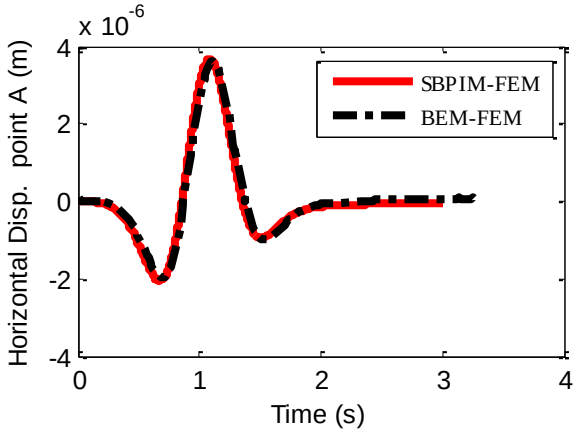

Fig.4. Horizontal displacement of point A due to the horizontal load R(t).

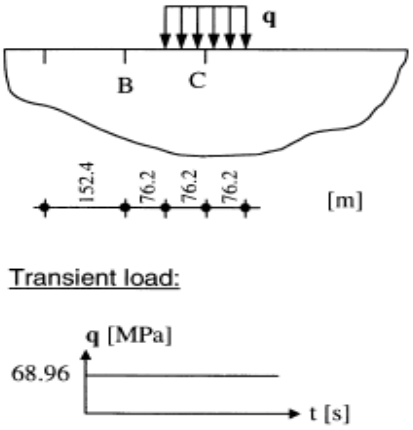

(a)

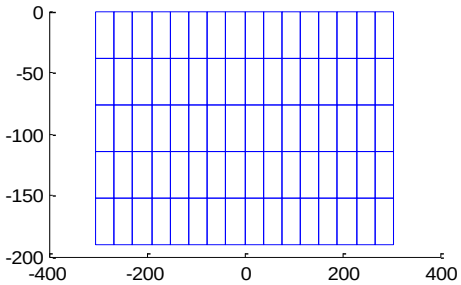

(b)

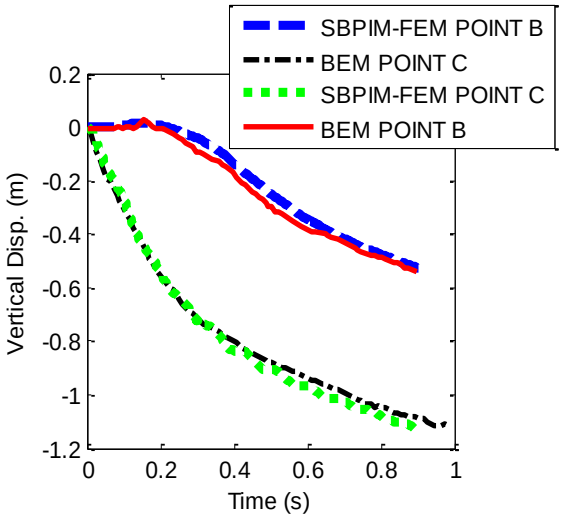

(c)

Fig. 5. (a) Considered rectangular soil medium and the applied load time history. (b) The finite element mesh used (c) Displacement time history of points B and C.

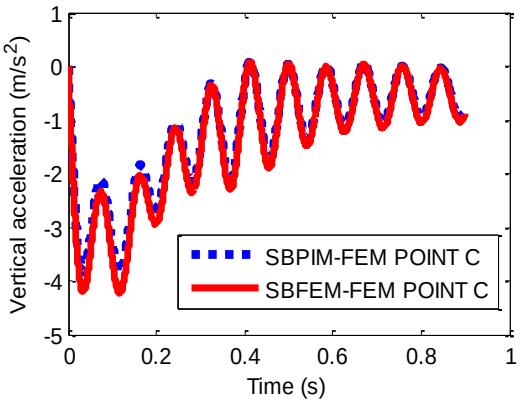

(a)

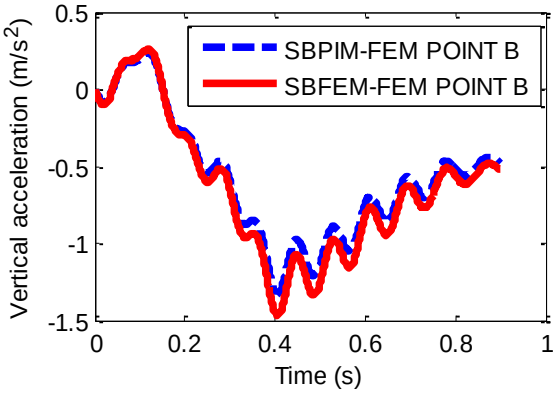

(b)

Fig. 6. (a) Acceleration time history of point C (b) Acceleration time history of point B.

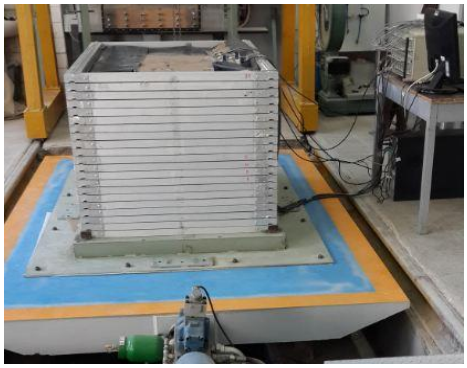

Fig. 7. Shaking table apparatus and the used shear box for experimental seismic response analysis of underground tunnel.

Fig. 8. The used aluminum box to model lining of tunnel

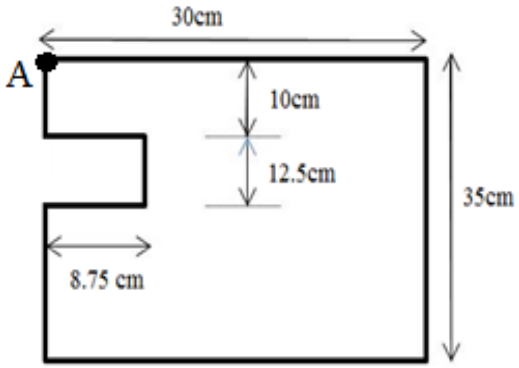

Fig. 9. Geometry of the system comprising of a rectangular tunnel and surrounding soil medium.

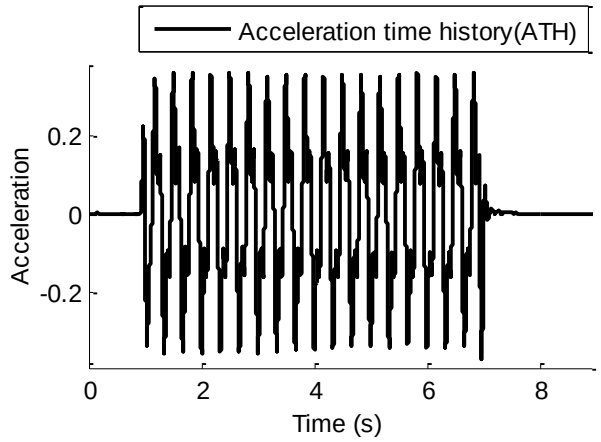

(a)

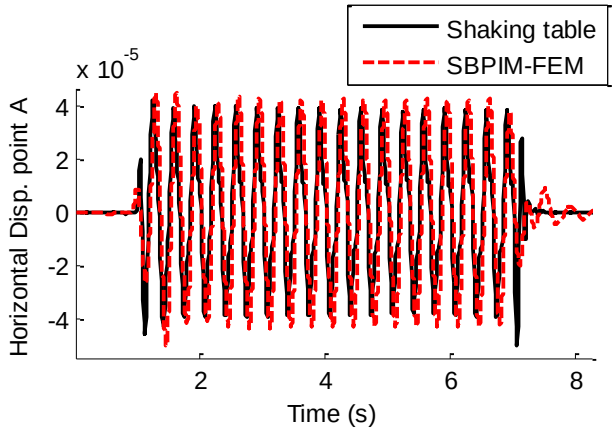

(b)

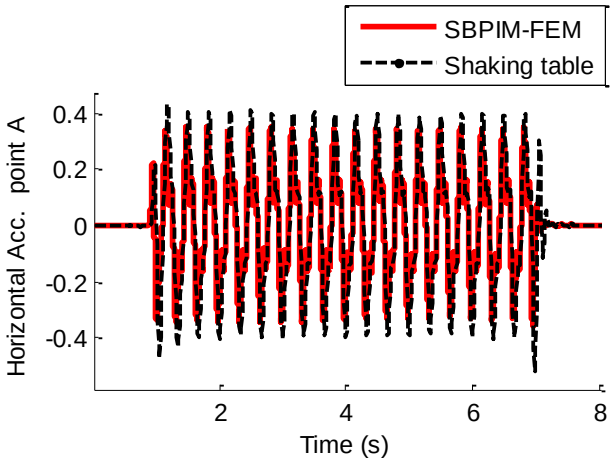

(c)

Fig. 10. (a) Acceleration time history of the applied vibration in the shaking table test. (b) Horizontal displacement of point A. (c) Horizontal acceleration of point A.

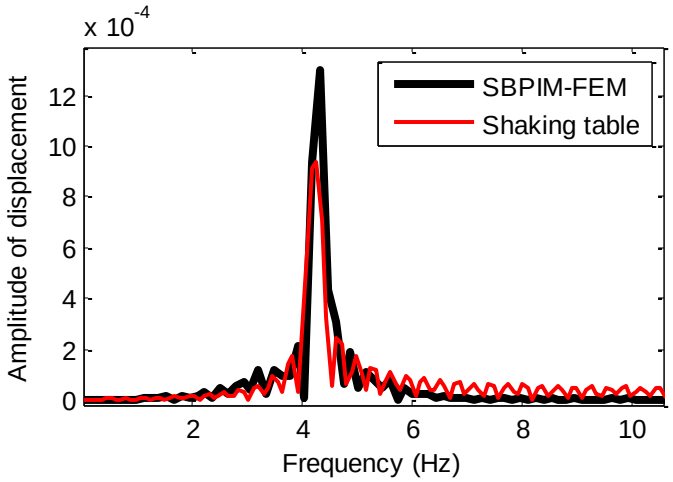

Fig. 11. Fourier amplitude of displacement of point A.

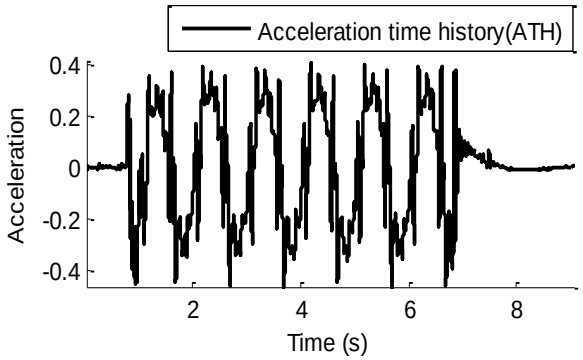

(a)

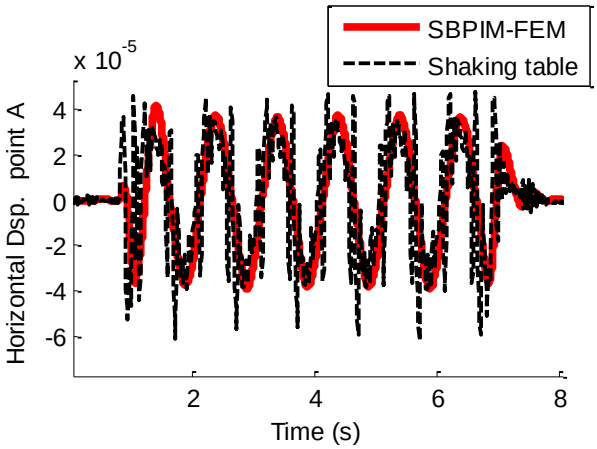

(b)

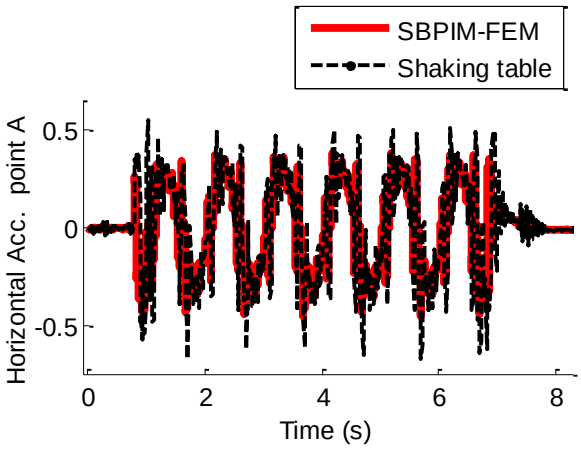

(c)

Fig. 12. (a) Time history of the selected acceleration. (b) Displacement time history of point A. (c) Acceleration time history of point A.

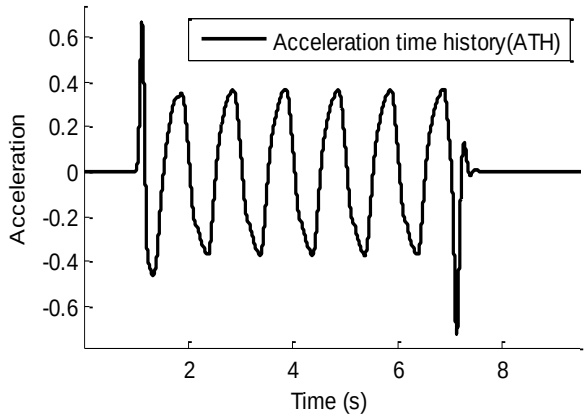

(a)

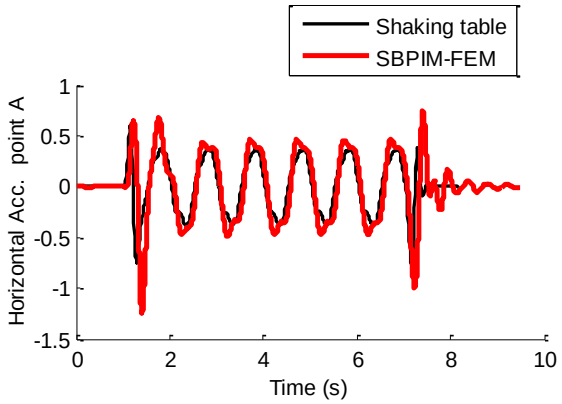

(b)

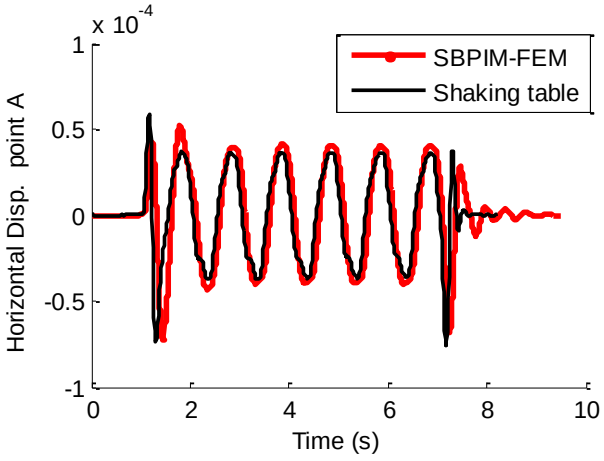

(c)

Fig. 13. (a) Time history of the selected acceleration for third verification. (b) Acceleration time history of point A. (c) Displacement time history of point A.